Visibility Calibrations With the Palomar Testbed Interferometer

A.F. Boden, M.M. Colavita, G.T. van Belle, M. Shao

Jet Propulsion Laboratory, California Institute of Technology,
4800 Oak Grove Drive, Pasadena, CA, 91109-8099

ABSTRACT

The Palomar Testbed Interferometer is a long-baseline, near-infrared astronomical interferometer capable of visibility measurement and narrow-angle differential astrometry. In this submission we consider the problem of fringe amplitude calibration as applied to the study of single and binary star systems with PTI. Methodologies for selecting appropriate calibration objects, and performing the calibrations to produce consistent multi-night datasets are considered. Applications of such calibrated datasets to binary orbit determination and stellar diameter measurements will be presented.

Keywords: interferometers, calibration

1. INTRODUCTION

The Palomar Testbed Interferometer (PTI) is a 110 m baseline K-band (2.0 – 2.4 μm) interferometer located at Palomar Observatory, and described in detail elsewhere, including a paper in these proceedings.[3,17] Among its operating modes, PTI measures visibility modulus squared, or V^2, of a brightness distribution on the sky. Such data can be used for many astronomical investigations, such as stellar diameter investigations,[9,5,14,15] dynamical studies such as binary star orbits,[11,7] and other resolution questions. The success of these programs often hinges on interpreting the raw data produced by the interferometer over an extended period of time, and in particular in the context of variable environmental and instrumental conditions.

The standard strategy for inter-relating visibility measurements over different epochs is to calibrate the measurements against a time-varying and possibly spatially-varying estimate of the *system visibility* V^2_{sys}, or the response of the interferometer to an unresolved point source.[9] In this way the calibrated science target visibility is an estimate of the target visibility that would have been measured by an ideal interferometer with similar physical parameters to the actual one. *A priori* the degree of variation in this system visibility estimate in time and sky position can be arbitrary depending on both instrumental and environmental conditions. Therefore the determination of an appropriate calibration strategy must be approached agnostically.

For long-baseline interferometers in general and PTI in particular, unresolved point sources do not exist because sources have finite surface temperature. Determinations of system visibility must thus be made with respect to sources of finite size. In principle any visibility-stable object (e.g. a single star at the resolution and sensitivity of the instrument) can serve as a calibration object. The calibration strategy may well hinge on the nature of the question being asked. For instance, if all that is desired is *precision* (repeatability) in the visibility measurements, then the diameter of the calibrator is relatively unimportant (although there are still higher-order baseline projection effects that must be considered). However, if one desires *accuracy* in the calibrated visibilities, the ability to produce such a dataset is limited by the accuracy and value of the model diameter for the calibration objects. Of course, relatively little is known about stellar diameters in general, and using model diameters for calibrators can lead to significant systematic errors in a calibrated dataset.

The most desirable calibrators have very high surface temperatures so as to have small angular size for a given brightness; this minimizes possible systematic errors resulting from using model diameters in calibration. This naturally leads one to consider early main-sequence stars as calibration objects, but such objects are rare compared with more evolved objects and late main-sequence stars in the PTI sky. It is further desirable to have the calibration objects have similar observing parameters (sky proximity, apparent brightness, time of observation) so as to minimize the possibility of temporal or proximity-related systematic effects. The desires to have calibrators with small angular sizes and be in close sky proximity to an arbitrary target are clearly at odds.

2. GENERAL ATTRIBUTES OF PTI VISIBILITIES

In his 1991 angular diameter paper, Mozurkewich discusses calibration of Mark III visibility measurements.[9] In that work he observes that Mark III system visibility estimates were "not a strong function of the time of night, or of position on the sky".* Given this experience it would be natural to assume the same to be true for PTI. However, there are important differences in the design of the two instruments. The most obvious difference is the collecting apertures: visibility measurements made with the Mark III were made through a 1 inch collecting aperture, a small fraction of an r_0 at 800 nm, while the limiting aperture at PTI is 40 cm, roughly one r_0 at K-band. There are also important differences in the mechanical mounts of the collecting siderostats, and differences in the seeing conditions at the Mt. Wilson and Mt. Palomar sites. It therefore behooves us to take an agnostic view of PTIs instrument performance with regard to temporal and spatial variation.

PTI is described in detail in the companion paper[17] but a few remarks about the instrument design and raw observables are in order. Like the Mark III, one half of the combined starlight beam is routed to a wide-band detector used for fringe tracking, while the second half of the combined beam is dispersed and detected in narrow-band spectral channels. Because of the narrow-bandwidth the spectral channels have a large coherence length ($\sim 75\ \mu$m), while the wide-band tracking channel has a significantly smaller coherence length ($\sim 15\ \mu$m). From the individual spectrometer channels we compute visibilities for a synthetic wide-band channel. This synthetic wide-band channel inherits the large narrow-band coherence length (and thus is not strongly affected by small fringe tracking errors), but otherwise has the attributes of a true wide-band channel. For science measurements we use only the spectrometer output and the synthetic wide-band channel derived from it.

2.1. Temporal Variation

Since many dynamical studies involve interpreting visibility time sequences to infer system parameters, it is important to quantify possible temporal variations of the instrument performance. Figure 1 shows four nights of raw data on two sources close to each other in the sky: HD 217014 – 51 Pegasi (inferred by Mayor & Queloz to have a planetary-mass companion by accurate radial velocity measurements,[10] and HD 215510. The two sources are 3.1 degrees apart in the sky, and have similar K-band brightness and expected apparent diameters. Per standard PTI operating procedure,[4] individual scans (fringe integrations roughly 2 minutes in duration) have been partitioned into 25 sec segments and averaged at the fringe phasor level. We have rendered the data points and error bars for a two minute scan as the averages and sample standard deviations for the 25 sec partitions. Beyond this averaging no additional processing has been performed on the data.

Figure 1 shows four nights of raw data on 51 Peg and HD 215510. Three of the nights (97216, 97236, and 97310) show visibility fluctuation in excess of the internal scatter of the measurements. This is typically the signature of multiplicity in the source; however, both objects seem to move in synchronism, suggesting in fact that the visibility changes are due to environmental or instrumental factors. This conjecture is bolstered by the fact that there are no known signatures for photometric variability or multiplicity in HD 215510. On the other night (97200), these same two objects exhibit roughly constant visibility profiles. In[1] we consider roughly twenty nights of data taken on these two objects, and find that the ratio of the visibilities are in fact stable with an RMS scatter of less than 3%, and that both stars are similarly stable with respect to a third calibration source. This leads to the conclusion is that the PTI system visibility can vary significantly on timescales of hours.

2.2. Spatial Variations

Unlike temporal variations, spatial variations are a bit more difficult to quantify without sources with known properties (e.g. accurate angular diameters for single stars). However, an interesting test of the stochastic portion of any instrumental effects can be made by calibrating 51 Peg with respect to a number of single calibration objects at a variety of sky separations. Presuming that 51 Peg has no luminous companions,[1,8,13] in the limit of similar calibrator brightness the noise around the best-fit single-star hypothesis is a measure of the calibration noise introduced by different calibrators. Table 1 lists the RMS scatter around the best-fit single-star hypothesis using a variety of stars as calibrators (and using calibration methods discussed in §3). Not surprisingly, the nearby calibrator (HD 215510) gives the best result (the lowest RMS scatter around the best-fit hypothesis). Interestingly, the results increase modestly as a function of sky separation with one marked exception (HD 222439), which results in residuals that are

*To be fair, Mozurewich et al separated contributions from the instrument and a separate seeing index, which certainly could be time-varying.

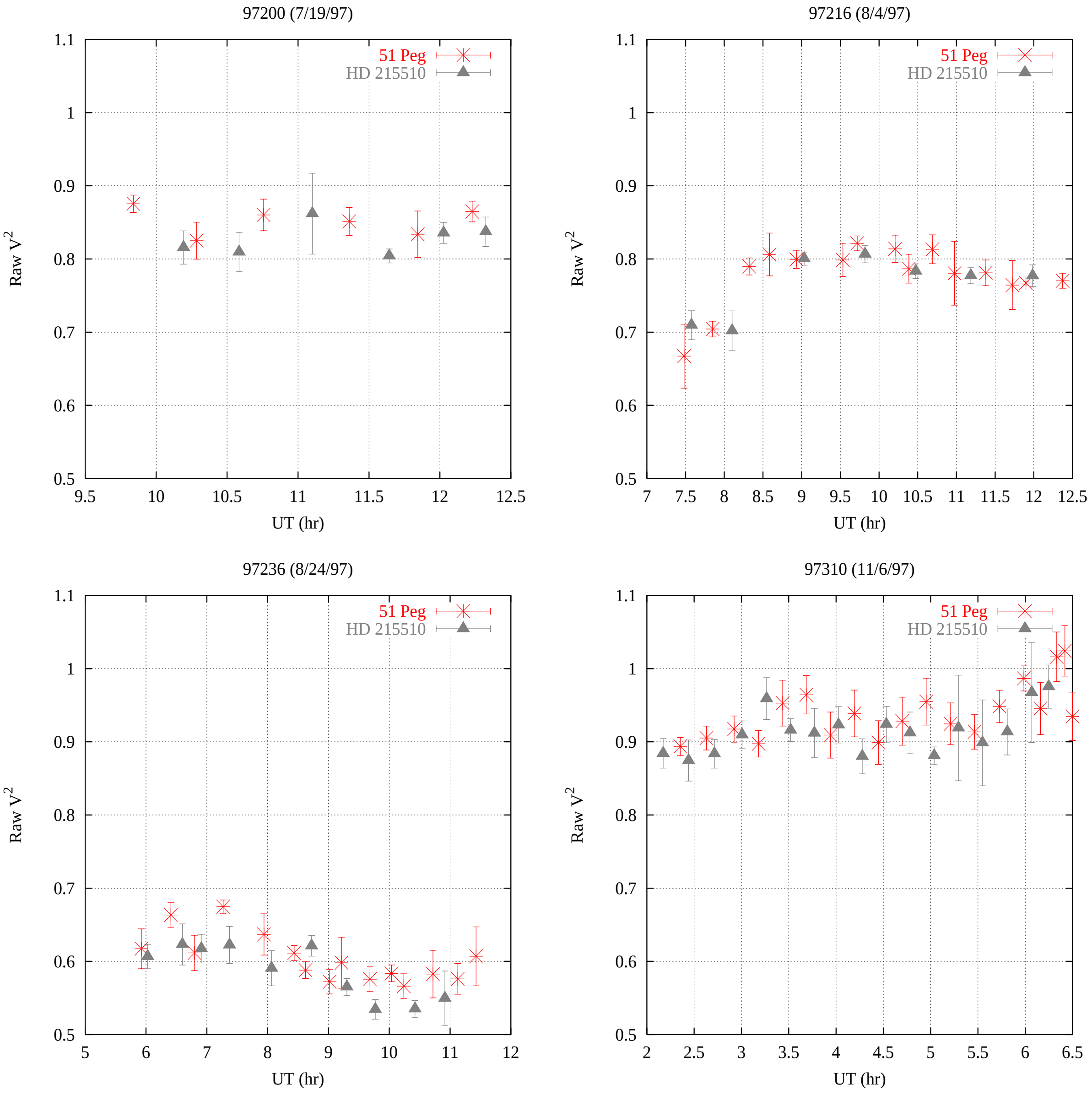

Figure 1. PTI Raw Data on Two Closely-Spaced Objects. The figure shows four nights of data on two adjacent objects: 51 Pegasi (HD 217014) and HD 215510. The two objects are separated by approximately 3.1° in the sky. On three of the four nights both objects exhibit formally significant (as inferred from the data's internal scatter – indicated by the error bars) excursions in the raw V^2 on time scales of hours. Yet both consistently to move in synchronism. This leads us to infer the excursions are due to instrumental or environmental factors.

Calibration Object	Est K Mag	Sky Separation From 51 Peg	N Samp	SS-Fit Resid RMS
HD 215510	3.9	3.1°	147	0.0295
HD 211006	3.4	13°	102	0.0390
HD 222439	4.2	25°	27	0.0739
HD 213558	3.7	30°	85	0.0432
HD 182488	4.5	49°	57	0.0505

Table 1. RMS Variations in 51 Peg Data Calibrated With Respect to A Variety of Calibration Sources. We have fit 51 Peg data calibrated by a number of calibrators at a variety of sky separation, and listed the RMS residuals in the calibrated data around the best-fit model. There is a clear correlation in the RMS residuals with sky separation in these data.

much larger than in the other examples. These results suggest that locality is a significant, though not overwhelming factor in the variation of PTI instrument performance.

3. CALIBRATION PROCEDURES

Calibration Computations Having observed general attributes of the PTI visibility data, it is straightforward to structure observing procedures and reduction methods to account for instrumental performance. We have constructed a computer code to calibrate science targets with respect to calibration objects using a variety of models for error propagation in time, sky proximity, and a similar variety of instrumental effects such as phase jitter and aperture intensity mismatch. This code has both Unix-style command line and web-browser user interfaces, to facilitate interaction for the spectrum of different PTI users.

The PTI calibration code performs data sorting, averaging, and comparison on selected objects. The user identifies a set of science targets to be calibrated, and a set of calibration objects to be used as references for the calibration. For the calibration objects, positions and model uniform-disk diameters (the calibration objects are assumed to be single stars) are required as input. The code selects calibration scans that are within user-defined temporal and possibly spatial constraints of a given science target scan, and estimates the system visibility, V^2_{sys}, for individual calibration scans based on the ratio of the measured and expected V^2 for the calibration object (see Figure 3). For potentially-resolved calibrators this expected V^2 calculation must include both wavelength and baseline projection effects. Multiple estimates of the system visibility from a single calibrator are weighted-averaged to determine a single system visibility estimate, and then estimates from multiple calibration objects are weight-averaged to compute a final ensemble system visibility estimate applied to the science target scan. During the multiple calibrator averaging system visibility estimates from individual calibrators are inter-compared for consistency and flagged or possibly rejected if they disagree beyond a user-defined consistency threshold. Uncertainties in the system visibility and the calibrated target visibility are inferred from internal scatter among the data in a scan, and standard error-propagation calculations. The calibration code can be used to calibrate a single night's data, or many nights of PTI data spanning an arbitrary length of time. There are versions of the calibration code that perform calibration of both the synthetic wide-band and individual spectrometer channel visibilities.

Figure 2 shows an example of the output of this calibration code on the same four nights of visibility data on 51 Peg given in Figure 1. As we asserted in §2, a calibration of this data considering both temporal locality and spatial locality results in a data set which is consistent with a simple interpretation for both objects, with a visibility value that is consistent on a night-to-night basis over 18 nights.[1]

Calibrator Selection Even with locality effects, it is formally sufficient to choose calibration objects that are arbitrarily resolved by the interferometer; so long as a consistent calibrator (ensemble) is used, a consistent reference exists for the calibrated data set. However, as presented above, a resolved calibration object will have an expected V^2 determined by its model parameters, e.g. the apparent diameter if we restrict ourselves to single stars. Even for single stars, an error in the model diameter manifests itself as systematic errors in the calibrated V^2 in two ways: in leading order there is global bias in the V^2 data, and in next-to-leading order there is an hour-angle dependent bias in computing the effects of the changing projected baseline length (Figure 3).

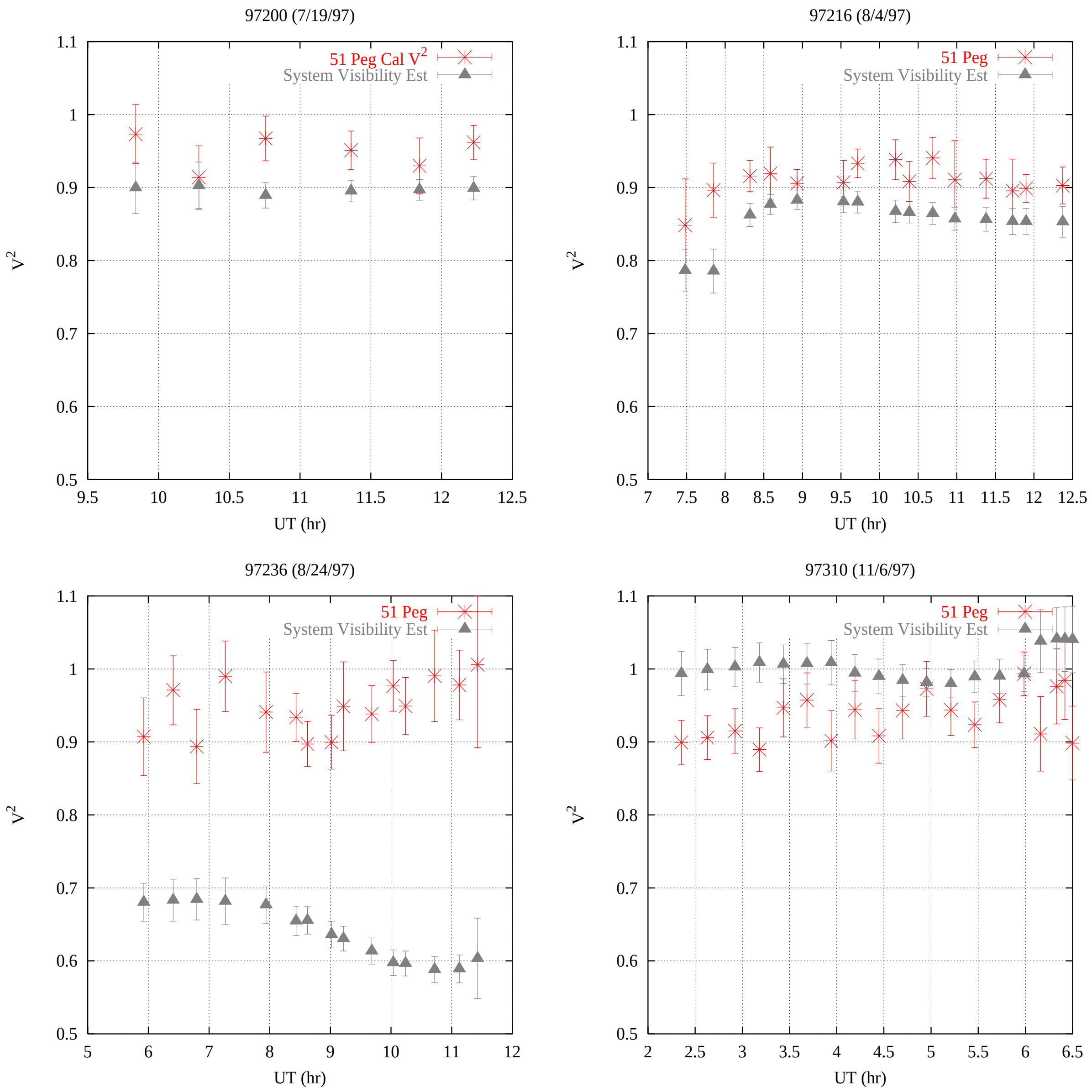

Figure 2. PTI Calibrated Visibility Data on 51 Peg. After Figure 1, taking a one-hour for the characteristic time scale over which instrumental or environmental effects can change, we have calibrated 51 Peg with respect to HD 215510. Calibrated data and the system visibility estimate for the four nights from Figure 1 are shown here.

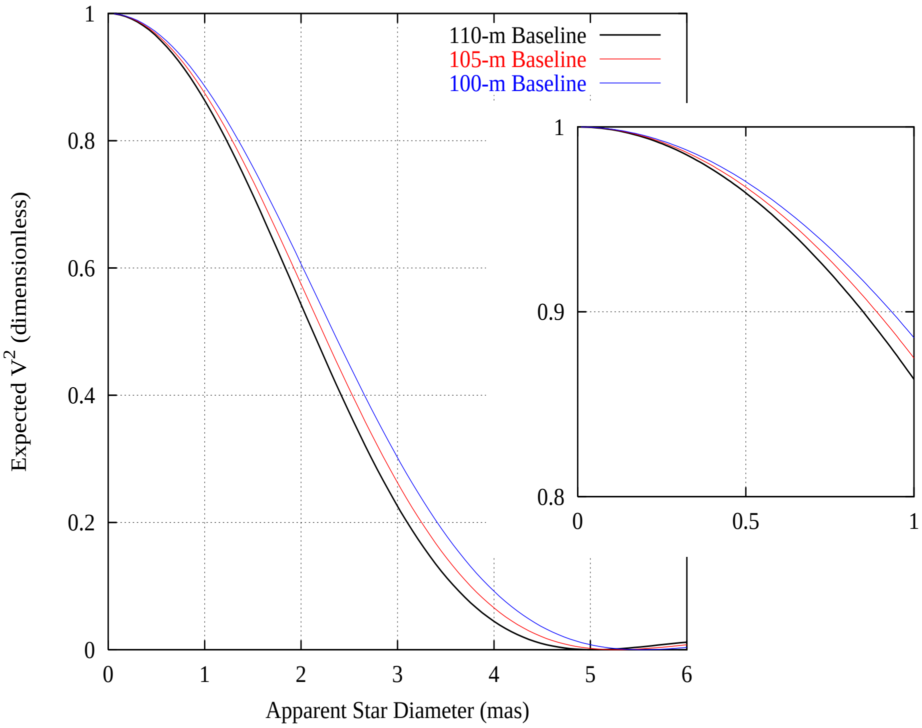

Figure 3. Expected Uniform Disk V^2 for the PTI N-S Baseline at 2.2 μm. Shown are expected uniform disk diameter V^2 curves for three representative projected baseline lengths (100, 105, and 110 m). Inset is a close-up of the region for diameters less than 1 mas, showing the reduction in variation of the expected V^2 with errors in the model diameter and projected baseline.

Of course, the best way of mitigating both of these effects is to chose calibrators that are unresolved by the interferometer, i.e. have nearly unit expected visibility. In this limit the expected V^2 becomes much less sensitive to errors in the calibrator model diameter (Figure 3). However, stars have finite surface temperature, and stars with smaller apparent diameters are generally dimmer than stars with larger apparent diameters. Thus PTI's sensitivity limits of about K $\sim$ 4.5[17] imposes significant limitations on calibrator selection, particularly if locality constraints are rigorously imposed.

Often, but not always, nearby (within 5 – 10°) main sequence stars with model apparent diameters below 0.8 mas can be found around an arbitrary science target. For such a calibration object the systematic calibration errors associated with a 10% error in the model diameter are approximately 1.7%. If such an object cannot be found we have taken to following a two-tiered calibration approach, relaxing the main sequence constraint and accepting more evolved objects as primary calibrators nearby the science target, and then augmenting the calibration set with secondary main-sequence calibrators drawn from a larger area (within 15 – 20°). So long as there are not strong sky-dependent biases in our instrument (something we can exclude at the 3% level from our ι Peg program[2] these secondary calibrators allow us to calibrate the apparent diameter of our evolved primary calibrators.

4. APPLICATIONS TO SCIENCE ANALYSES

Giant Star Diameters A standard topic addressed by long-baseline interferometers is the determination of apparent diameters for stars. PTI has studied a large number of giant and supergiant stars in 1997, and estimated their angular diameters based on visibility calibration techniques described here. In multi-night fits to diameters for these stars van Belle et al 1998 finds night-to-night repeatability at the 0.015 (1.5 %) level in V^2.[16]

Figure 4 gives an example from our giant star program. The plot gives effective temperatures as a function of the V - K color index for $\sim$ 120 giant stars with angular diameters estimate from PTI and IOTA observations. The

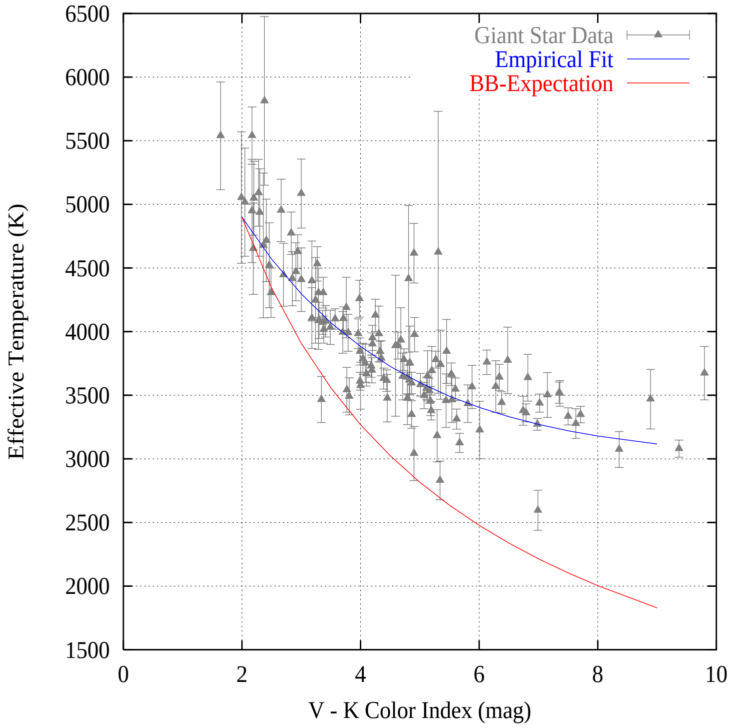

Figure 4. Effective Temperature vs. V - K Color Index For Giant Stars Based on 1997 PTI Data and Previously Published IOTA Data. This graph shows the effective temperature estimated from apparent diameter and bolometric flux of a sample of $\sim$ 120 giant stars (of which $\sim$ 70 were measured by PTI in 1997) with apparent diameters measured by PTI and IOTA. The data indicates a striking departure from black-body expectations as the objects become more red (from van Belle et al 1998 in prep).

angular diameter data is combined with bolometric flux estimates derived from archival photometry to estimate the effective temperature, and then plotted against the V - K index. The giant stars in this sample show a significant departure from black-body expectations as the star becomes more red (increasing V - K).

Binary Orbits Another traditional "bread-and-butter" science topic for long-baseline interferometers such as PTI is the measurement of visual orbits of binary stars. At PTI we have studied the visual orbits of a number of binary systems. One of these systems, ι Pegasi (HD 210027), is depicted here in Figures 5 and 6. As first noted by Fekel & Tomkin,[6] the circular orbit of ι Peg is nearly eclipsing, yet no evidence for eclipses have been seen in repeated photometric studies of the system.[2] Our visual orbit does not in fact predict eclipses: based on our best-fit model the inclination and component diameters the possibility for eclipses in the system is excluded at high confidence.

Figure 6 shows a comparison of seven consecutive nights (12 Aug – 18 Aug 1997) of calibrated V^2 data on ι Peg, and the best-fit model V^2 prediction for the system over that same period. Inset in a frame below are the residuals between calibrated data and model. The calibrated data is in excellent agreement with the V^2 predictions from the best-fit model: the average absolute deviation between model and data is 0.014 (1.4%) in 112 calibrated scans over 17 nights.[2]

5. SUMMARY

We have review some of the basic attributes of PTI data, and techniques we have developed for its calibration. These techniques, when applied to science analyses result in datasets with internal scatter at or below the 2% level.

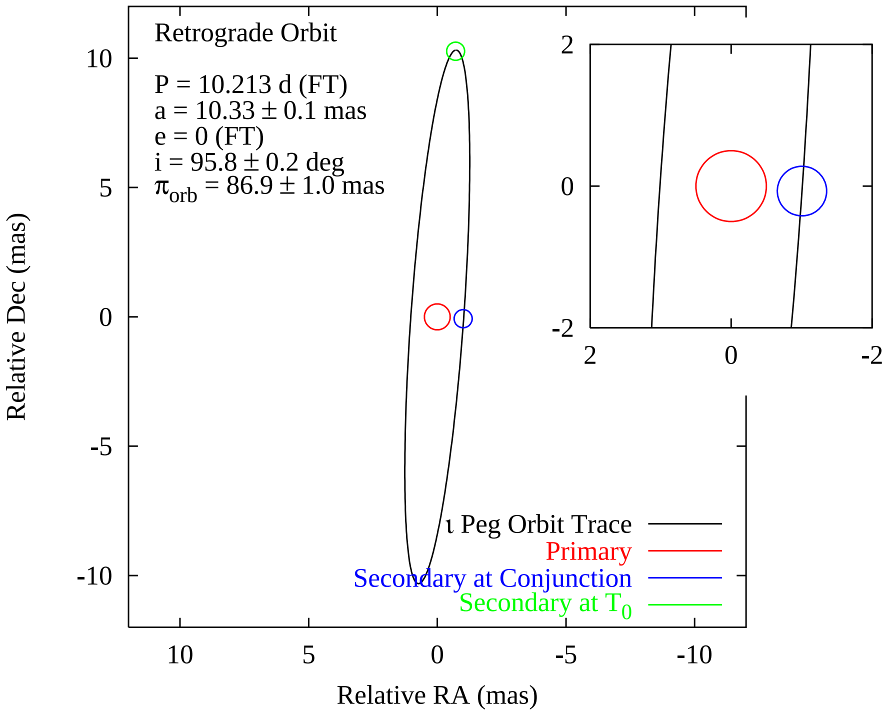

Figure 5. Visual Orbit for the Binary System ι Pegasi From PTI V^2 Measurements. Shown is the apparent motion of the G8V secondary around the F5V primary. Combined with an accurate spectroscopic orbit from Fekel and Tomkin,[6] our visual orbit results in very precise mass estimates for the two components.[2] Inset we show the two components at conjunction. According to our best-fit model for the system the two stars pass within ~ 0.2 mas of apparent limb-to-limb contact, but do not in fact eclipse.[2]

Acknowledgements

The work described in this paper was performed at the Jet Propulsion Laboratory, California Institute of Technology under contract with the National Aeronautics and Space Administration.

REFERENCES

1. Boden, A.F. et al (The PTI Collaboration) 1998a, "An Interferometric Search for Luminous Companions to 51 Pegasi", ApJL in press (astro-ph/9804016).
2. Boden, A.F. et al (The PTI Collaboration) 1998b, "The Visual Orbit of ι Pegasi", ApJ submitted.
3. Colavita, M.M. et al 1994, "ASEPS-0 Testbed Interferometer", Proc. SPIE 2200, 89 – 97.
4. Colavita, M. et al 1998, PASP in prep.
5. Dyck, H.M., Benson, J.A., van Belle, G.T., and Ridgway, S.T. 1996, "Radii and Effective Temperatures for K and M Giants and Supergiants" AJ 111, 1705-1712.
6. Fekel, F. and Tomkin, J. 1983, "The Double-Lined Spectroscopic Binary Iota Pegasi", PASP 95, 1000 – 1005.
7. Hummel, C. et al. 1995, AJ 110, 376.
[Marcy et al 1997]
8. Marcy, G.W. et al. 1997, "The Planet Around 51 Pegasi" ApJ 481, 926.
9. Mozurewich, D. et al, "Angular Diameter Measurements of Stars" AJ 101, 2207.
10. Mayor, M. and Queloz, D. 1995, "A Jupiter-Mass Companion to a Solar-Type Star", Nature 378, 355.
11. Pan, X. et al 1990, "Apparent Orbit of the Spectroscopic Binary Beta Arietis with the Mark III Stellar Interferometer", ApJ 356, 641.

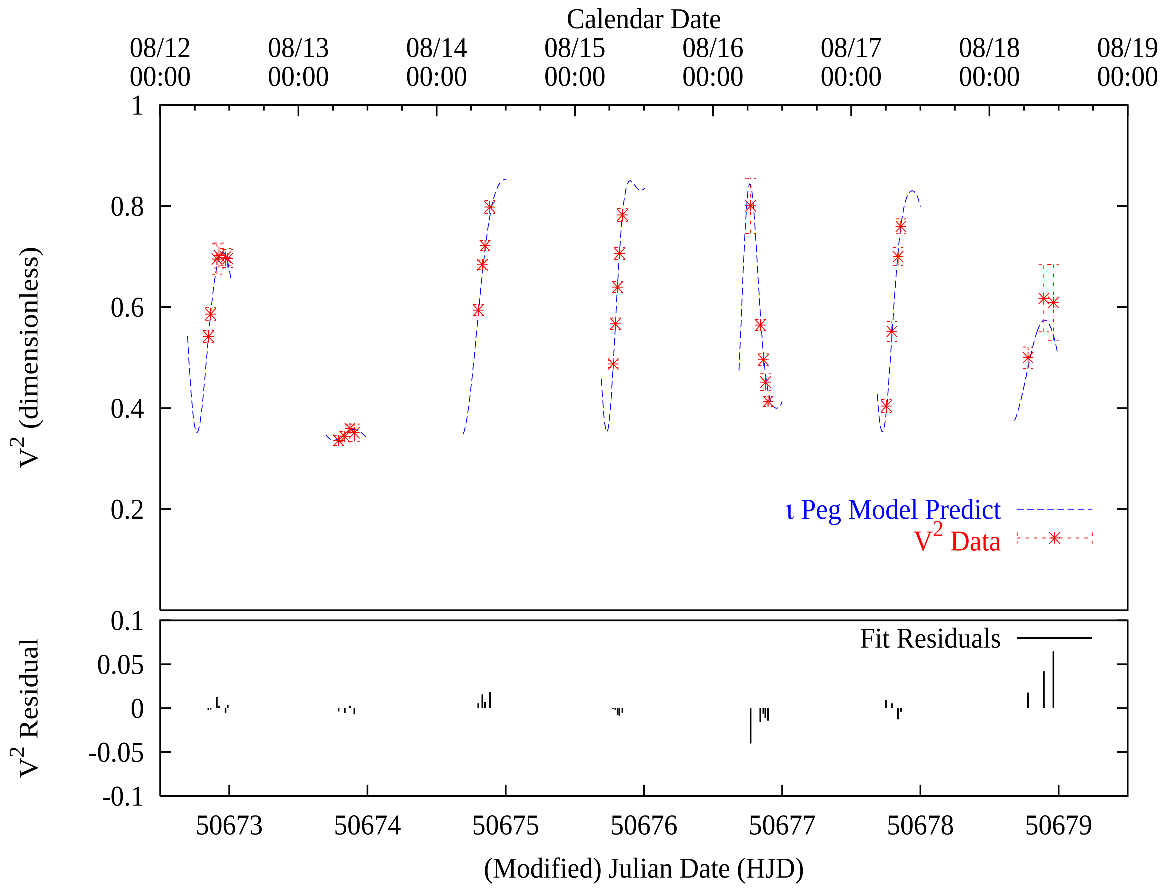

Figure 6. Seven Nights of Calibrated V^2 Data on ι Peg Compared to the Best-Fit Model for the System. Shown here is seven nights (12 Aug – 18 Aug 1997) of data on ι Peg compared with the V^2 predictions given by the best-fit model for the system. Inset in a frame below are the residuals between calibrated data and model. The average absolute deviation between model and data is 0.014 (1.4%) in 112 calibrated scans over 17 nights.[2]

12. Perryman, M.A.C. et al 1997, "The Hipparcos Catalogue", A&A 323, L49 – L52.
13. Pravdo, S., Angelini, L., Drake, S., Stern, R., and White, N. 1996, "The X-ray Evidence that the 51 Peg Companion is a Planet", New Astron. 1, 171 – 176.
14. Quirrenbach, A., Mozurkewich, D., Buscher, D.F., Hummel, C.A., and Armstrong, J.T. 1996, "Angular Diameter and Limb Darkening of Arcturus" A&A 312, 160.
15. van Belle, G.T., Dyck, H.M., Thompson, R.R., Benson, J.A., and Kannappan, S.J. 1997, "Angular Size Measurements of Carbon Miras and S-Type Stars", AJ, 114, 2150.
16. van Belle, G.T. et al (The PTI Collaboration), BAAS 191,# 46.01.
17. Wallace, K. et al 1998, "The Palomar Testbed Interferometer", these proceedings.